Directed evolution for cell separation in budding yeast

Benjamin Galeota-Sprung[1a], Erik Pritchard[1], Crystal Huang[1], Amy Fernandez[1], and Paul Sniegowski[1]

[1] University of Pennsylvania
[a] Corresponding author

Abstract

Haploid and diploid natural isolates of the yeast *Saccharomyces cerevisiae* were evolved under a daily transfer protocol that selected against clumpy growth and for cell separation. For the haploid populations, whole genome sequencing revealed strong selection to deactivate *AMN1*, a known regulator of cell separation, recapitulating evolution that likely occurred during the domestication of common lab strains. We also observed multiple mutational hits to the Rim101 pathway, which was not expected. Mutations to both *AMN1* and the Rim101 pathway were strongly associated with cell separation. In the diploid populations, we observed the parallel emergence of a large partial deletion of chrIII, the so-called Hawthorn's deletion. We show that this deletion is associated with reduced clumpy growth. The mechanism by which Hawthorne's deletion affects cell separation is unknown but may be related to an effect on budding pattern.

Introduction

Cell aggregation phenotypes in the yeast *S. cerevisiae* phenotypes include flocculation, pseudohyphal growth, invasive growth, biofilms, and clumpy growth (Soares, 2011). Clumpy growth (sometimes called chain formation (Stewart, 2009)), is a phenomenon in which growing cells do not fully separate after budding, leading to clusters of related cells. In contrast to clumpy growth, flocculation is reversible, fast-acting, and not dependent on relatedness. Typical laboratory strains of yeast are not clumpy, with much of the variation in clumpiness across strains explained by different alleles of the cell separation regulator *AMN1* (Li *et al.*, 2013). In contrast to laboratory strains, wild isolates of *S. cerevisiae* are often clumpy growers, especially as haploids (Fig. 1). Wild strains tend to be more robust than lab strains in many respects, including faster growth rate, higher sporulation efficiency, and lower rate of petite production (Dimitrov *et al.*, 2009). One barrier to the use of wild strains in laboratory work is that their clumpiness can make some otherwise routine assays—for example dilution plating to obtain colonies and flow cytometry of single cells—challenging or complicated. Evolution experiments in which selection pressure is applied to an aggregation phenotype have been carried out (e.g. Ratcliff *et al.*, 2015; Hope *et al.*, 2017) but so far as we are aware all such experiments to date have selected for increased aggregation. Here we report the results of an evolution experiment in which we selected for *non*-clumpy growth. We evolved replicate populations of haploid and diploid strains, derived from wild isolates, for 57 days under a daily transfer protocol that selected against large clumps and for separated cells. Across populations, we found genetic parallelisms at the level of gene, pathway, and macromutation.

Methods

Strains

The diploid strain YPS602 is a monosporic isolate of YPS133, which was isolated from Tyler Arboretum, Pennsylvania, as described previously (Sniegowski, Dombrowski and Fingerman, 2002); similarly, the

closely related diploid strain YPS602 is a monosporic isolate of YPS142, also isolated from Tyler Arboretum. Both strains are related to the more widely known YPS 128, and are members of the North American Oak clade (Peter *et al.*, 2018). YPS2070 is a haploid *MATα* heterothallic *(ho::kanMX)* derivative of YPS602 and YPS2055 is a haploid *MATa ho::kanMX* derivative of YPS606.

Media and growth conditions

In the evolution experiment, growth occurred in glass 50 mL Erlenmeyer-type flasks containing 10 mL synthetic dextrose (SD) medium supplemented with ampicillin and tetracycline, at 30 degrees C and shaken at 200 rpm. SD was chosen as the media for the experiment because the ancestral diploid strain was not clumpy in YPD after the exponential growth phase.

Evolution experiment

4 replicate cultures of each of the strains YPS602 (diploid), YPS 606 (diploid), YPS2055 (*MATa* haploid), and YPS2070 (*MATα* haploid) were founded and transferred daily according to the following protocol: a 2 mL aliquot of well-mixed culture were removed to a small glass tube and allowed to settle undisturbed for 10 (Day 1 – Day 8), 20 (Day 9 – Day 14), or 30 (Day 15 – Day 66) minutes. After the waiting period, 100 uL of culture was carefully removed from near the top of the culture aliquot and transferred to 9.9 fresh media in a new flask.

Daily transfers were performed for 57 days. At regular intervals, the number of cells transferred was estimated by hemocytometer count. Also at regular intervals, 3 mL of culture was frozen in 30 % glycerol and stored at -80 C. Clonal isolates were obtained from frozen population samples by streaking. For the control (no selection against clumping) evolution experiment, conditions were identical except that 50 ul of well-mixed culture was added to 9.95 mL fresh media, and the evolution was carried out for 66 days.

Populations analyzed

After completion of the experiment, we discovered that the diploid YPS606-founded populations been inadvertently discontinued and replaced with YPS2055-founded populations at some point after Day 29 and before Day 35; in other words, the 4 YPS2055 populations were each accidentally duplicated. We therefore adopted the following numbering scheme to distinguish populations. The haploid populations H1, H2, H3, and H4 were founded from YPS 2070 and the haploid populations H5a, H5b, H6a, H6b, H7a, H7b, H8a, H8b were founded from YPS 2055, with the a/b scheme signifying the culture duplication event. Population H4 was not analyzed due to a separate technical error; therefore after 57 days of evolution there were 11 haploid populations available for analysis. The diploid populations D1, D2, D3, and D4 were founded from YPS 602 and evolved for 57 days. The diploid populations D5, D6, D7, and D8 were founded from YPS 606 and evolved for 29 days.

Whole-genome sequencing

We used the genome assembly of YPS128 (also a member of the North American Oak clade) as provided by (Yue *et al.*, 2017) as the reference genome for all sequencing described here. For clones, a culture started from a frozen chunk, while for frozen populations, the entire frozen sample was thawed and 10 ul used to inoculate a new culture. After growth overnight, DNA was extracted from 1 mL of culture using kit D7005 from Zymo Research. Reads were mapped to the reference genome using `bwa`, and duplicate reads removed by `PicardTools MarkDuplicates`. Mutations were called using `freebayes` on the default settings, with all potential variants reviewed manually and examined in IGV. Plots of read depth were created in R from the output of `samtools -depth` and used to locate chromosomal deletions. Results from this pipeline were spot-checked using `breseq`.

Settling and sedimentation assays

To produce indirect measurements of the degree of clumpy growth, we quantified the settling of cultures. When a culture of yeast is allowed to settle, two features are naturally apparent to an observer: (1) sediment collects at the bottom of the culture vessel and (2) the culture suspension moves visibly downwards, replaced by clear media. We measured both of these manifestations of settling. Clones were started from a frozen chunk and grown overnight in YPD, and then grown for two 24h cycles in SD (diluted 1/100 at each transfer) before assay. In the sedimentation assay, 5 mL of well-mixed culture was placed into a 15 mL conical tube suspended vertically; after two hours, the amount of sediment at the bottom was measured. In the settling assay, 900 ul of culture was briefly spun down (90 s at 10,000 rcf) and resuspended in 900 ul sterile water, 700 ul of this resuspension was pipetted into a narrow-profile cuvette and allowed to settle. The resuspension step was necessary because cultures in SD do not settle evenly. After two hours the position of the point at which the liquid visible transitioned from clear to cloudy was measured.

While diploid strains are far less clumpy in YPD than in SD, for haploid strains the reverse is true: they are clumpier in YPD than SD. Coupled with the fact that cultures are a good deal denser in YPD, this makes changes to settling and sedimentation easier to observe in YPD than SD. Thus, although the evolution experiment was carried out in SD, for haploid strains we carried out settling and sedimentation assays in YPD. For these assays, both sedimentation and settling measurements were taken from the same 5 mL of culture in a 15 mL conical tube; the settling line in these cases was estimated as the midpoint between clear media and cloudiest culture.

Microscopy and cluster size analysis

To produce direct measurements of the distribution of cluster sizes in diploid strains, we employed the following procedure. A frozen chunk of the strain of inoculated an overnight culture in YPD; the following day this culture was transferred to SD diluting 1/100 and allowed to grow for 24 h; then another 1/100 dilution and growth cycle in SD was performed; and finally on the 4th day 200 ul of culture was transferred to 12 mL fresh SD and grown until A600=0.6, at which point photographs of the culture were taken at 400x magnification. Subsequently, the number of cells in each cluster was manually labelled (Supplemental Fig. 7) and recorded.

Sporulation and tetrad dissection

Sporulation and tetrad dissection were carried out by standard methods.

Results

Evolution in haploid populations produced parallel changes at the gene and pathway level

All clones isolated from haploid Day 57 populations were clearly less clumpy when examined microscopically (illustrative examples in Fig. 1B), and displayed changes of large magnitude in our bulk property assays (Fig. 2). Whole-genome sequencing revealed that all clones had either a mutation to *AMN1*, a known regulator of cell separation, or a gene in the Rim101p pathway: *RIM8, RIM13, RIM20, or RIM101*. There were no *AMN1* / Rim101p double mutants. Of 6 independent *AMN1* mutations, 4 seemed to be obvious loss-of-function mutations (nonsense or frameshift). While there was no suggestion in the data that the substitutions to *AMN1* had a lesser effect than the frameshifts and nonsense mutations, we performed allele replacement assays on these isolated, replacing AMNC452Y and AMN1L472P with the ancestral allele. These replacements completely restored the clumpy phenotype (Supplemental Fig. 1). Similarly, the Rim101 pathway mutations include one substitution and the rest are frameshift or nonsense mutations.

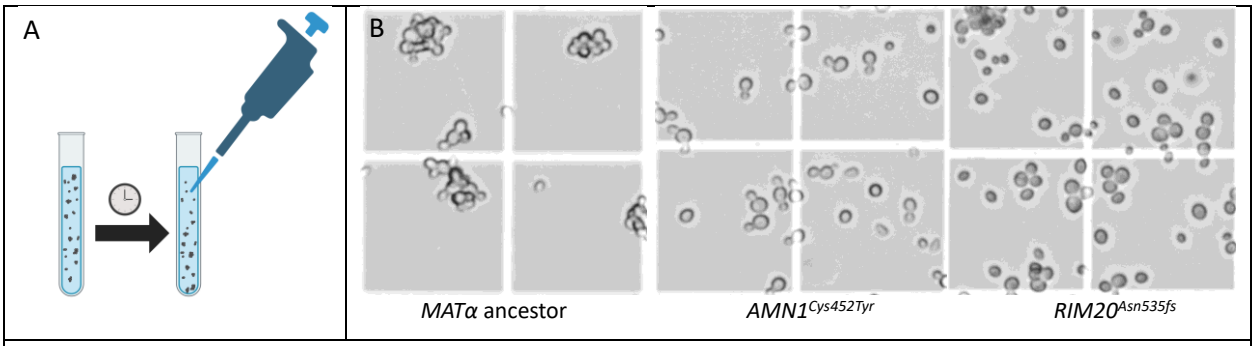

C

Gene	Haploid population 1	2	3	5a	5b	6a	6b	7a	7b	8a	8b
AMN1	C452Y	S498fs	K315*		L472P	R446*		D373*	D373*		
RIM8										S354fs	
RIM13							Q110*				
RIM20				N535fs							
RIM101											C184F
STE11									C430*	K236fs	S630Y

Figure 1. (A) The transfer regime selected for well-separated cells, as large clusters tend to settling out. (B) The ancestral haploid strain is a clumpy grower; evolved clones with mutations to AMN1 and RIM20 are far less clumpy. (C) Across 11 haploid populations, parallel changes at the gene (*AMN1*, *STE11*) or pathway (Rim101) level were observed.

We also observed three independent mutations to *STE11*. These all appeared in conjunction with an *AMN1* or Rim101p pathway mutation. We confirmed that these clones are sterile (do not mate), as expected. Because populations H7a and H7b were once a single population and share the mutation $AMN1^{D373*}$, we can infer with relative confidence that the $ste11^{C430*}$ mutation arose in a background that already had $AMN1^{D373*}$. The *ste11* mutations appear then to always be second mutations. Our settling and sedimentation assays do not pick up an effect of knocking out *STE11* (Supplemental Fig. 2); however, there is a subtle visual difference in settling appearance (data not shown).

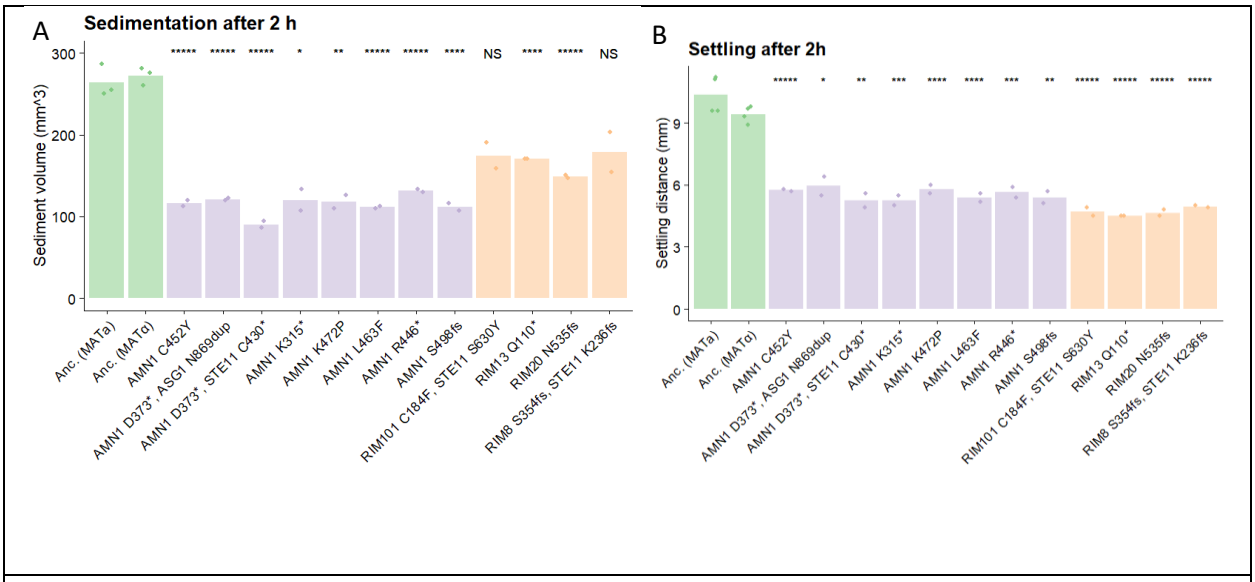

Figure 2. Evolved haploid strains have bulk properties consistent with more cell separation: (A) less sediment at the bottom of a tube after a defined period of settling; and (B) for those cells still in suspension, less visible progress downwards.

Haploid populations were diverse and experienced soft sweeps

We noticed that most pairs of clones isolated from populations that were originally a single population do not share the same mutation (true for H5a and H5b; H6a and H6b; H8a and H8b; but not for H7a and H7b). This suggested that populations were diverse, with many contending lineages. To confirm this we performed whole-population sequencing of two haploid populations. The results (Table 1) confirmed our hypothesis; we detected at least 4 independent *AMN1* or Rim101p mutant lineages in each population. We suspect that the multiple competing *AMN1* mutations are essentially neutral with respect to one another, and that one or another would eventually fix only by drift; however it seems more probable that there is a fitness difference between *AMN1* and Rim101p that would cause one or the other to deterministically fix, given enough evolution time. However, we have been unable to detect any such difference to date (data not shown).

Haploid pop. H3		Haploid pop. H5a	
Mutation	**Freq**	**Mutation**	**Freq**
AMN1 K315*	0.60	RIM20 N535fs	0.43
AMN1 L463F	0.12	AMN1 Q224*	0.24
AMN1 R162*	0.10	RIM8 A>C 409,048	0.08
AMN1 E476*	0.06	RIM8 T>C 409,518	0.04
AMN1 L473P (TG>CT)	0.04		
AMN1 L391S	0.03		

Table 1. Whole population sequencing of two Day 57 haploid populations.

A dominant mutation produces less clumpy growth in diploids

In one of the four Day 57 diploid populations, the representative clone that we isolated had only one apparent mutation, a nonsynonymous heterozygous mutation to the voltage-gated calcium channel gene *CCH1*. This isolate sedimented significantly less than the ancestor and was quantitatively less clumpy (Fig. 4). We sporulated and dissected tetrads of this isolate to produce F994L/F994L and F994F/F994F homozygotes, the genotypes of which were confirmed by Sanger sequencing. The homozygous mutant had a similar less clumpy phenotype to the heterozygous mutant (Supplemental Fig. 5), suggesting that this mutation is dominant.

A large deletion of chr III evolved multiple times in diploid populations

We found that a large deletion on chromosome III evolved repeatedly in diploid populations. Whole-population sequencing of population D1 revealed that this macromutation was fixed or nearly fixed. We also found evidence for this deletion in 3 of 4 Day 29 populations (D5, D6, and D8; see Supplemental Fig. 8), meaning that this deletion was observed in 6 of 8 diploid populations. This deletion spans the region from MAT to HMR, or, in one case, the region from MAT to HML (Fig. 3).

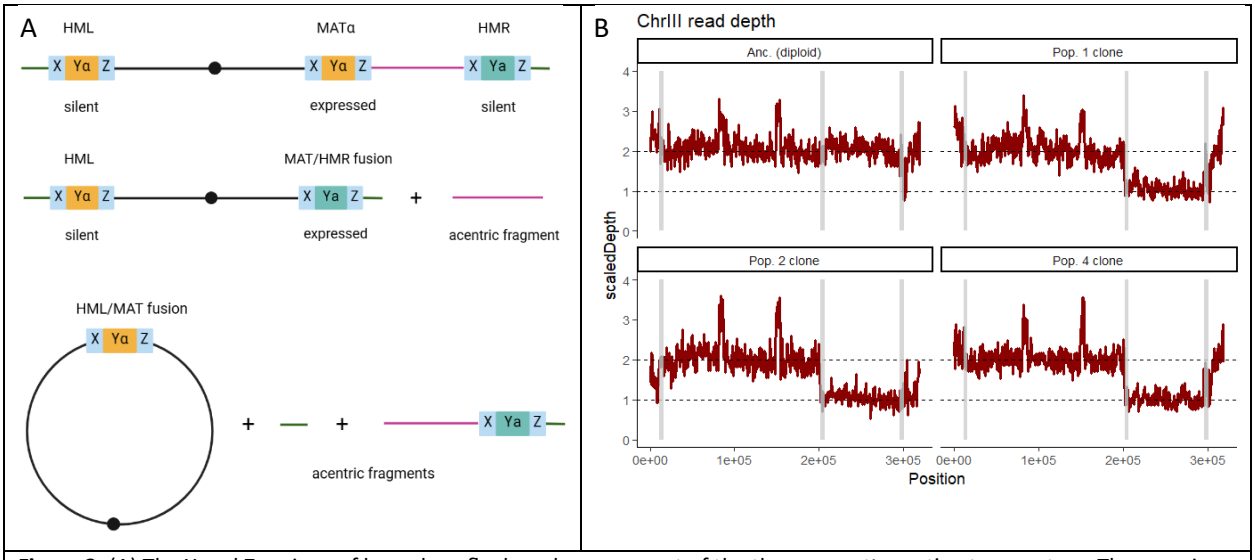

Figure 3. (A) The X and Z regions of homology flank each component of the three-cassette mating type system. These regions of homology can lead to the formation of aberrant fusions. The MAT-HMR fusion causes a large deletion; the MAT-HML fusion causes an even larger deletion and leads to a ring chromosome. (B) Representative clones from 3 of the 4 diploid cultures evolved for 57 days. Two are heterozygous for a MAT-HML fusion and one is heterozygous for a MAT-HMR fusion.

This deletion is historically known as Hawthrone's deletion and its observation had an important role in the working out of the *S. cerevisiae* mating-type switching system. It is surprising to find evidence for its positive selection. Clones with one of these deletions displayed substantially less sedimentation (Fig. 4a) and a quantitative imaging assay showed that they are less clumpy than the ancestor (Fig. 4b). For example, the ancestral proportion of cells occurring in clumps of 4 cells or fewer was 43%; for the Hawthorne's deletion strains, this estimate ranged from 65% to 77%.

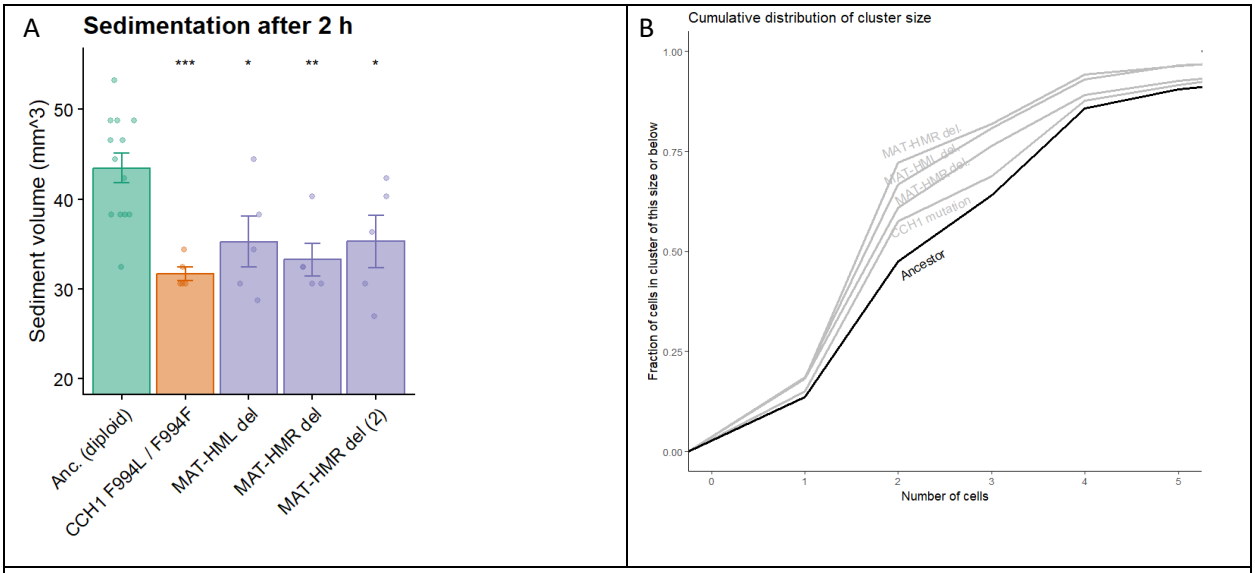

Figure 4. (A) Evolved diploid clones show significantly less sedimentation than the ancestral diploid. (B) While visual microscopic inspection of evolved diploid clones does not show an obvious phenotype, a quantitative investigation revealed that the distribution of cell cluster size is markedly altered.

The MAT-HMR region includes several essential genes. Thus, we expected the deletion strains to segregate 2:2 live:dead when sporulated and dissected, and this was the case (Supplemental Table 2). The two live spores yielded diploid colonies homozygous for chrIII with the ancestral sedimentation phenotype (Supplemental Fig. 4), indicating that indeed the deletion causes the phenotype.

One curiosity was that the isolate with the MAT-HML fusion would be expected to have a ring chromosome III (Fig. 3a); and we would expect this ring to further depress spore viability below 50%, since crossovers during meiosis between the ring and the linear homolog could generate aberrant products. Yet, we found no evidence of a depression in spore viability, which led us to question whether there truly was a ring. Therefore, we performed long-read sequencing. A substantial fraction of long reads mapped to regions left of MAT *and* right of HML (Supplemental Fig. 6), indicating that the ring-generating fusion occurred as suspected. We saw no evidence, from the long-read data, of a breakage anywhere else, leaving the lack of depression in spore viability as something of a mystery.

Discussion

This evolution experiment yielded outcomes both predictable and surprising. How *AMN1* regulates (prevents) cell separation in haploids was nicely dissected by Fang *et al.* (2018). Semi-inadvertent selection for *AMN1* mutants is likely part of the evolutionary history of common lab strains. This experiment has perhaps recapitulated that selection; thus it is not surprising that we recovered many *AMN1* mutants. It is a demonstration of the power of experimental evolution to aid in genotype-to-phenotype mapping (given that a selection gradient relevant to the phenotype of interest can be applied) that had we *not* known about *AMN1*'s role in governing cell separation, this experiment would have clearly pointed towards it.

The multiple hits to the Rim101 pathway are less expected. That pathway is known to have a role in pH sensing (Yan *et al.*, 2020) and regulation of cell size (Shimasawa *et al.*, 2023), and to connect to pathways regulating filamentous growth (Cullen and Sprague, 2012). Yet a role in cell separation during normal physiological growth conditions has not previously been elucidated—perhaps because many lab strains are already well-separated.

One motivation for this experiment was to test for differences in the genetic architecture of adaptation between diploids and haploids. We hypothesized that haploids would evolve mainly by loss-of-function mutations, while diploids would tend to evolve by gain-of-function mutations. Indeed, all causative mutations that we found in haploids appear to be loss-of-function, disabling the function of *AMN1*, the Rim101 pathway, and *STE11*. We found only one nonsynonymous mutation, in *CCH1*, that putatively causes more cell separation in diploids, and it does indeed appear to be dominant which at least suggests that it is a gain-of-function mutation, although we have not yet established that as fact.

The most surprising outcome was repeated selection for MAT-HMR or MAT-HML deletions on chromosome III. Such deletions, historically known as Hawthorne's deletion, were instrumental in the long and distinguished effort to work out the mating type switching system (Hawthorne, 1963; Haber, Rogers and McCusker, 1980; Herskowitz, 1988; Haber, 1998). It is interesting that we have observed these deletions in completely wild-type diploids, separately from any context of mating type *switching*, as the ancestral diploid was *MATa/MATα* and the deletion strains remain *MATa/MATα*. It is possible that the initial deletion event caused a switch that led to a transient *MATa/MATa* or *MATα/MATα* state. We are not sure why these deletions cause more cell separation, but we guess that it may be related to apparent haploinsufficiency of *BUD23* and/or *BUD31*. Mutants of both of these genes are known to display random budding patterns, and we find that our deletion strains, which have only one copy of each, have a more disordered budding pattern than their ancestor (Supplemental Table 1). However, this could be an unrelated effect of the deletion.

The repeatability of the deletion suggests that it is always happening at some low rate. This points to a previously unknown additional cost or load of maintaining the three-cassette mating type system. Such a load would join a long list of the various costs of sexual reproduction that are rather mysteriously tolerated by eukaryotic populations.

Supplemental Figures and Tables

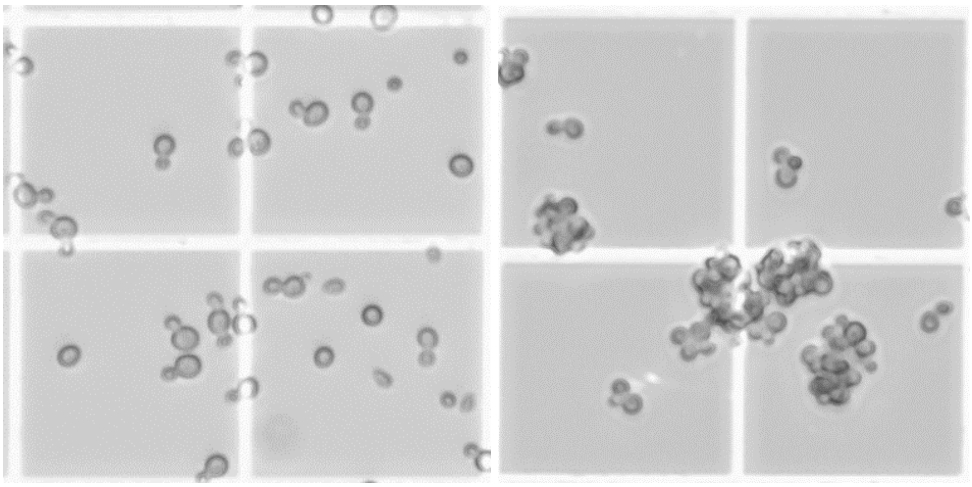

AMN1^{Cys452Tyr} *ΔAMN1*^{Cys452Tyr}*::AMN1*^{Anc}

Supplemental Figure 1. Replacement of an evolved *AMN1* missense allele with the ancestral allele completely restores the clumpy phenotype.

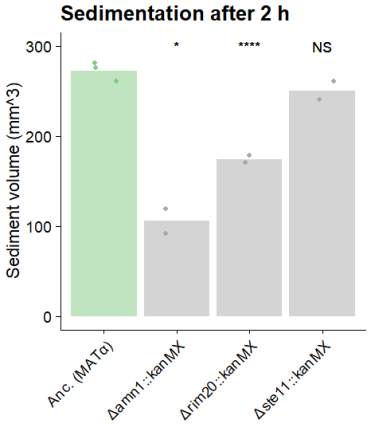

Supplemental Figure 2. We did not detect an effect of knocking out *STE11*.

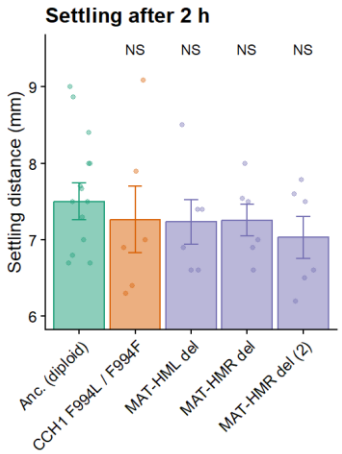

Supplemental Figure 3. Settling (as opposed to sedimentation; see Fig. 3) assays in the diploid were noisy and no significant effects were found, although the mean effect was in the expected direction.

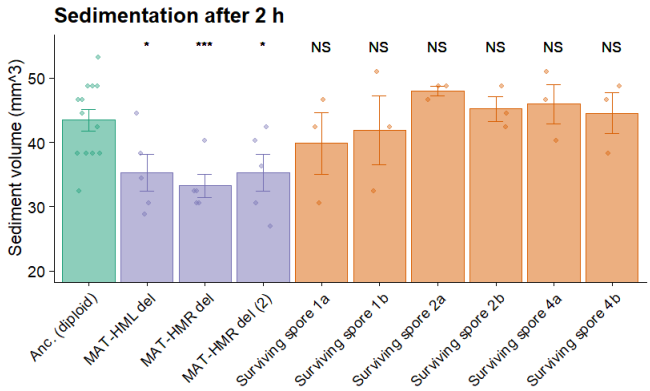

Supplemental Figure 4. Strains with chrIII MAT-HML or MAT-HMR deletions segregate 2:2 live dead. The two living dissection products (which are homozygous for complete chrIII) revert back to the ancestral sedimentation phenotype.

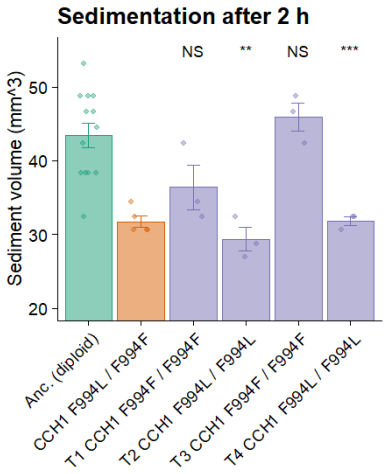

Supplemental Figure 5. Sedimentation assay of dissected sporulation products of the diploid that acquired the *CCH1* F994L mutation. The results demonstrate that (1) the phenotype goes with the mutation and (2) the effect appears to be dominant, i.e. the homozygote does not have a more extreme phenotype than the heterozygote.

A

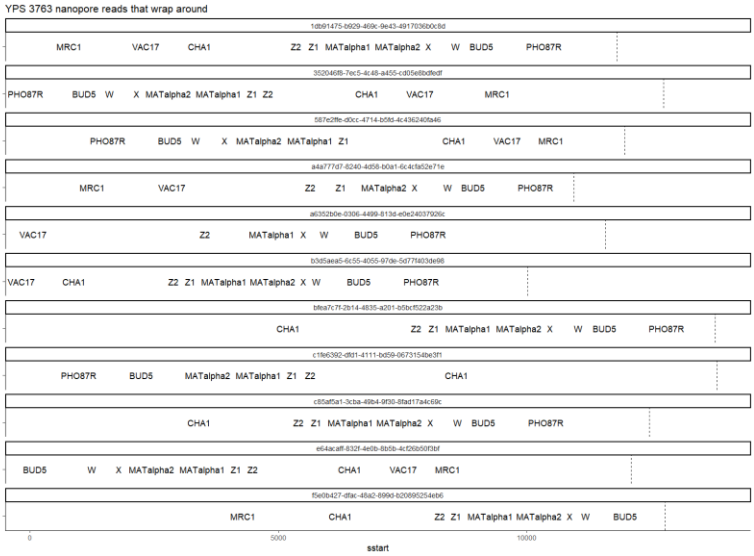

B

Reads >= 10 kb	
Spanning HML	7
Spanning MAT	18
HML-MAT fusion	11

Supplemental Figure 6. Long-read (Nanopore) sequencing evidence of a ring chromosome III. (A) Individual long reads with BLAST hits left of HML (MRC1, VAC17, CHA1) and right of MAT (BUD5, PHO87). (B) The number of long reads that support an HML-MAT fusion is about equal to the number of long reads that canonically span HML or MAT, supporting the notion of that the strain is heterozygous for the deletion.

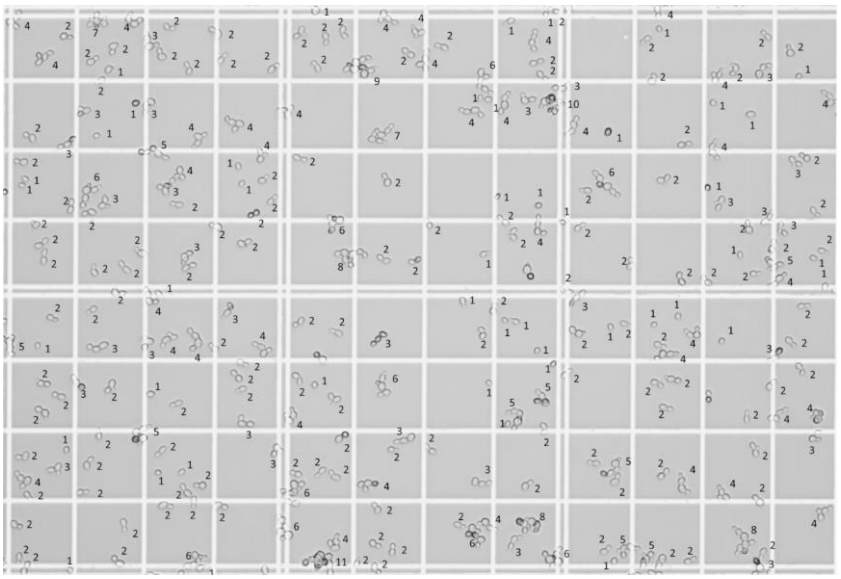

Supplemental Figure 7. A sample image that has been labelled for cluster size.

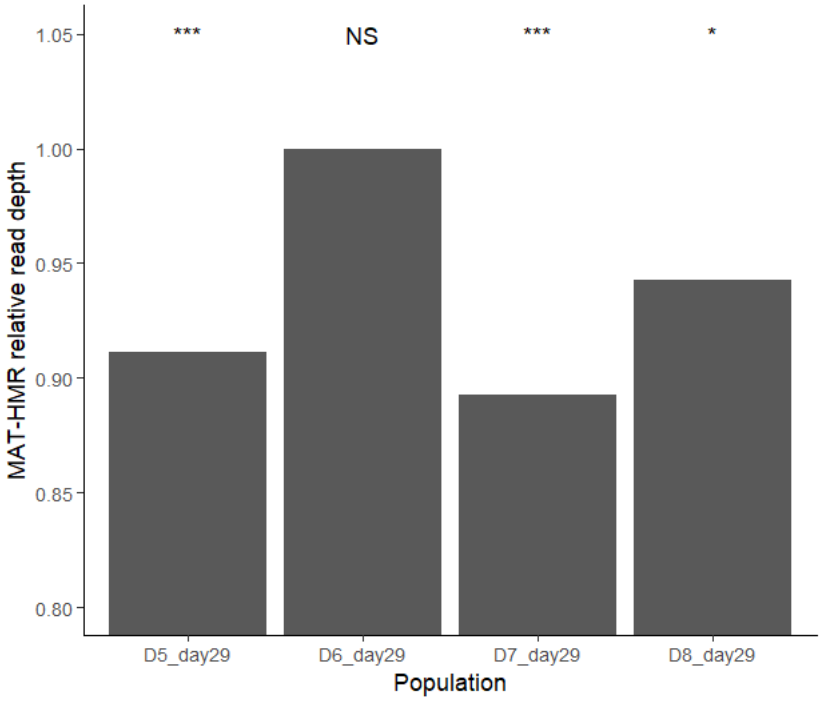

Supplemental Figure 8. Three of the four diploid populations halted at Day 29 (D5, D7, and D8) show evidence of a low-frequency lineage with a chrIII MAT-HMR deletion.

Budding polarity

Strain	Alternating pole	Same pole	Ratio
Diploid ancestor	48	23	2.1
MAT-HML fusion	31	29	1.1 ** (p <0.01)
MAT-HML fusion (2)	32	25	1.3 * (p <0.05)
MAT-HMR fusion	32	27	1.2 ** (p <0.01)

Supplemental Table 1. The chrIII deletions affect budding polarity. From photographs taken at 400x magnification, diploid mothers were scored for the site of emergence of their last two daughters.

	Surviving spores per tetrad				
	1	**2**	**3**	**4**	**Total viability**
MAT-HMR fusion	1	9	0	0	0.48
MAT-HMR fusion (2)	0	13	0	8	0.69
MAT-HML fusion	1	18	2	0	0.51

Supplemental Table 2. Spore viability of the chrIII deletion isolates.

References

Cullen, P.J. and Sprague, G.F. (2012) 'The Regulation of Filamentous Growth in Yeast', *Genetics*, 190(1), pp. 23–49. Available at: https://doi.org/10.1534/genetics.111.127456.

Fang, O. *et al.* (2018) 'Amn1 governs post-mitotic cell separation in Saccharomyces cerevisiae', *PLOS Genetics*, 14(10), p. e1007691. Available at: https://doi.org/10.1371/journal.pgen.1007691.

Haber, J.E. (1998) 'Mating-Type Gene Switching in Saccharomyces Cerevisiae', *Annual Review of Genetics*, 32(1), pp. 561–599. Available at: https://doi.org/10.1146/annurev.genet.32.1.561.

Haber, J.E., Rogers, D.T. and McCusker, J.H. (1980) 'Homothallic conversions of yeast mating-type genes occur by intrachromosomal recombination', *Cell*, 22(1, Part 1), pp. 277–289. Available at: https://doi.org/10.1016/0092-8674(80)90175-0.

Hawthorne, D.C. (1963) 'A Deletion in Yeast and Its Bearing on the Structure of the Mating Type Locus', *Genetics*, 48(12), pp. 1727–1729.

HERSKOWITZ, I. (1988) 'The Hawthorne Deletion Twenty-Five Years Later', *Genetics*, 120(4), pp. 857–861.

Hope, E.A. *et al.* (2017) 'Experimental Evolution Reveals Favored Adaptive Routes to Cell Aggregation in Yeast', *Genetics*, 206(2), pp. 1153–1167. Available at: https://doi.org/10.1534/genetics.116.198895.

Li, J. *et al.* (2013) 'Polygenic Molecular Architecture Underlying Non-Sexual Cell Aggregation in Budding Yeast', *DNA Research*, 20(1), pp. 55–66. Available at: https://doi.org/10.1093/dnares/dss033.

Peter, J. *et al.* (2018) 'Genome evolution across 1,011 Saccharomyces cerevisiae isolates', *Nature*, 556(7701), p. 339. Available at: https://doi.org/10.1038/s41586-018-0030-5.

Ratcliff, W.C. *et al.* (2015) 'Origins of multicellular evolvability in snowflake yeast', *Nature Communications*, 6(1), p. 6102. Available at: https://doi.org/10.1038/ncomms7102.

Shimasawa, M. *et al.* (2023) 'The pH-sensing Rim101 pathway regulates cell size in budding yeast', *Journal of Biological Chemistry*, 299(3). Available at: https://doi.org/10.1016/j.jbc.2023.102973.

Sniegowski, P.D., Dombrowski, P.G. and Fingerman, E. (2002) 'Saccharomyces cerevisiae and Saccharomyces paradoxus coexist in a natural woodland site in North America and display different levels of reproductive isolation from European conspecifics', *FEMS Yeast Research*, 1(4), pp. 299–306. Available at: https://doi.org/10.1111/j.1567-1364.2002.tb00048.x.

Soares, E.V. (2011) 'Flocculation in Saccharomyces cerevisiae: a review', *Journal of Applied Microbiology*, 110(1), pp. 1–18. Available at: https://doi.org/10.1111/j.1365-2672.2010.04897.x.

Stewart, G.G. (2009) 'The Horace Brown Medal Lecture: Forty Years of Brewing Research', *Journal of the Institute of Brewing*, 115(1), pp. 3–29. Available at: https://doi.org/10.1002/j.2050-0416.2009.tb00340.x.

Yan, H. *et al.* (2020) 'The pH-sensing Rim101 pathway positively regulates the transcriptional expression of the calcium pump gene PMR1 to affect calcium sensitivity in budding yeast', *Biochemical and Biophysical Research Communications*, 532(3), pp. 453–458. Available at: https://doi.org/10.1016/j.bbrc.2020.08.083.

Yue, J.-X. *et al.* (2017) ‘Contrasting evolutionary genome dynamics between domesticated and wild yeasts’, *Nature Genetics*, 49(6), pp. 913–924. Available at: https://doi.org/10.1038/ng.3847.